

# An Empirical Approach to Estimate the Reliability of LEDs as Components of Military Equipment

Q. Tiep La\*, D. Vališ, and Z. Kohl

*Faculty of Military Technology, University of Defence, Brno, Czech Republic*

The manuscript was received on 12 November 2025 and was accepted after revision for publication as an original research paper on 7 February 2026.

## **Abstract:**

*Military equipment is highly specialized and integrates advanced technologies to operate reliably in complex environments. Light-emitting diodes (LEDs) are increasingly used in military systems due to their superior performance, long lifetime, and high reliability, making their reliability critical to overall system effectiveness and combat capability. This study proposes an empirical framework for estimating LED reliability using accelerated reliability testing combined with statistical analysis, explicitly linking test conditions to actual operating conditions. The methodology follows a structured, stepwise procedure encompassing test design, data acquisition, and reliability estimation. It is applied to LEDs subjected to frequent ON/OFF cycling, yielding robust estimates of the lifetime distribution, survival function, and cumulative hazard function.*

## **Keywords:**

*military equipment, LED, accelerated testing, reliability estimation, lifetime estimation, survival function, cumulative hazard function*

## **1 Introduction**

Military technical equipment integrates high-density, high-tech systems to perform specialized tasks under extremely harsh conditions, including wide variations in temperature, humidity, chemical exposure, mechanical stress, and radiation. To meet combat requirements, such equipment must comply with strict technical standards, ensuring high reliability, long-term stable operation, rapid response, maintainability, and minimal risk during missions [1, 2]. Consequently, the research and development of military systems are accompanied by comprehensive evaluation programs and rigorous reliability testing under conditions simulating actual battlefield environments [1, 3, 4], following international and military standards, such as [1–7].

---

\* Corresponding author: Faculty of Military Technology, University of Defence, Kounicova 156/65, CZ-662 10 Brno, Czech Republic. E-mail: quoctiep.la@unob.cz. ORCID 0000-0002-4809-737X.

Light-emitting diodes (LEDs) are increasingly used in modern military equipment due to their efficiency, longevity, durability, and ability to operate under harsh conditions. They serve as core lighting components in tactical lights, signaling systems, cockpit displays, night vision devices, optical navigation, and target recognition systems. Ensuring LED reliability directly affects the overall performance, availability, and maintenance optimization of military equipment. In this study, we focus on LEDs as key components of military systems.

Evaluating LED reliability is a critical challenge, especially since LEDs are dual-use devices, blurring the boundary between military and civilian applications. A general approach applicable to both domains is therefore necessary. Traditional methods for estimating LED reliability include mathematical, physics-based, and numerical techniques. While these approaches can provide useful insights, they often require deep understanding of underlying physical, chemical, and material processes and may carry significant uncertainty [8]. For example, Cu et al. [9] assessed reliability of LEDs in military vehicles based on the existing standard, while Kyatam et al. [10] and Tsai et al. [11] applied numerical simulations (ANSYS and OQB-LEDsim) to study degradation under varying operating conditions.

Data-driven methods offer a highly accurate alternative by extracting reliability information directly from controlled test data. Testing under normal operating conditions is realistic but impractical for long-life, high-reliability LEDs due to long durations and high cost. Accelerated testing (AT) addresses these limitations by exposing devices to elevated stress conditions, such as higher temperature, increased current, compressed duty cycles, or faster switching, thereby accelerating degradation and reducing test time [12]. AT is typically classified into Accelerated Life Testing (ALT), which collects failure-time data, and Accelerated Degradation Testing (ADT), which continuously tracks performance degradation. Existing standards provide guidance for AT planning and execution. IEC 62506:2023 [13] outlines general methodologies, IES LM-80 [14] defines lumen depreciation measurement, TM-21 [15] specifies extrapolation for long-term lumen maintenance, and MIL-HDBK-217F [6] details reliability prediction for military electronic components. In AT, stress types and profiles are diverse, encompassing environmental and operational factors with step, ramp, constant and cyclic profiles [16]. Based on the applied stress, the relationship between accelerated life and real operating life is typically modelled through life-stress relationships such as the Arrhenius model, Inverse Power Law, or other physics-informed models [17]. These models enable the extrapolation of test results under high-stress conditions to predict device reliability under normal usage.

At this point, detailed analyses are required regarding (1) ATs for LEDs, including test conditions, equipment, and collected parameters, and (2) methods used to estimate lifetime from ADT data. Herzog et al. [18] conducted ADTs on 312 high-power LED modules under different thermal stresses and constant current based on LM-80 guidelines, collecting optical data and estimating Mean Time to Failure (MTTF) using the Arrhenius model. Meanwhile, Singh et al. [19] tested 40 OSRAM Yellow Dragon LEDs under combined temperature-humidity stress at 85 °C and 85 % RH in both ON and OFF conditions. A temperature-humidity chamber, current source, and spectroradiometer were used to monitor lumen degradation. In another aspect, Truong et al. [20] tested GaN LEDs at two high-temperature levels for 1 500 hours with a constant 350 mA current. A climate chamber, spectrometer, and IR camera recorded spectral intensity and surface temperature. A random diffusion model was then applied to estimate lifetime, and the results were compared with TM-21 predic-

tions. In parallel, Choi et al. [21] stressed package LEDs at high temperature, with some in constant-ON mode and others in 60-s ON / 260-s OFF cycles. Brightness was recorded during cooling using a T3Ster system, while junction temperature was monitored by IR camera. Ibrahim et al. [22] evaluated InGaN LED lamps under constant thermal stress using a thermal chamber, an IR camera, and an integrating sphere to record photometric parameters. Lifetime was estimated using a Gamma process and a Bayesian network. Vališ et al. [23] performed step-thermal ADT ( $60\text{ }^{\circ}\text{C} \rightarrow 70\text{ }^{\circ}\text{C} \rightarrow 80\text{ }^{\circ}\text{C} \rightarrow 90\text{ }^{\circ}\text{C}$ ) while voltage was monitored and applied a stochastic diffusion model for lifetime prediction. A similar approach was used in [24] for medical LEDs. Wang et al. [25] designed ADTs for UVC LEDs stressed at 30 mA, where one group was irradiated with a  $^{60}\text{Co}$   $\gamma$ -ray source (1.35 MeV), reaching a total 1 750 krad(Si) dose, enabling comparison of radiation-induced degradation. In addition, many ADTs have been conducted under different stress conditions to investigate lumen depreciation [26, 27], and several studies reflect real operation modes such as ON/OFF cycling [28] and PWM control [29].

The above analysis confirms the importance of reliability assessment and lifetime prediction for LEDs used in military applications. Reliability testing plays a central role in collecting degradation data and forms the foundation for data-driven predictive models. Existing standards provide general procedures for performing such tests. However, most studies focus only on applying standard AT protocols, where stress conditions are selected based on predefined stress types. Although some works consider real operating modes, they often do not clearly justify the chosen test regime or demonstrate how it reflects actual field operation. These limitations indicate a lack of empirical, application-oriented testing frameworks that explicitly link test design, real-world operating conditions, and data-based reliability estimation. Motivated by these gaps, the paper proposes an empirical approach to reliability estimation for LEDs used as military equipment. The main contributions are as follows:

- an empirical approach for constructing a reliability test regime that reflects real operating conditions of LEDs in military systems, including test setup, data collection, and data processing,
- an ALT is performed using existing laboratory equipment, where we clearly justify the selection of stresses, operating modes, and test parameters, demonstrating how they relate to real conditions,
- a statistical data-driven method for processing degradation data, estimating lifetime distribution, survival function and cumulative hazard function, and extracting useful information that can serve as the basis for technical assurance and maintenance planning.

The remainder of this paper is organized as follows. Section 2 presents the experimental approach for reliability estimation. Section 3 provides a detailed case study applying the proposed methodology. Finally, Section 4 summarizes the main conclusions of this study.

## 2 An Empirical Approach to Estimating the Reliability of LEDs

In this section, we present an empirical approach for estimating the LED reliability. The overall flowchart of the proposed methodology is shown in Fig. 1. The approach is structured into three main phases: pre-test, test, and post-test. Each phase plays a critical role in lifetime estimation: the pre-test phase defines the test conditions, stresses, and monitoring parameters based on device specifications and operating con-

ditions to ensure meaningful and relevant data; the test phase executes the accelerated lifetime or degradation tests, generating the necessary reliability data under controlled conditions; and the post-test phase involves statistical, data-driven analysis to process the collected data, extract degradation trends, and estimate lifetime parameters. For clarity, the methodology is presented as a sequence of specific steps within each phase.

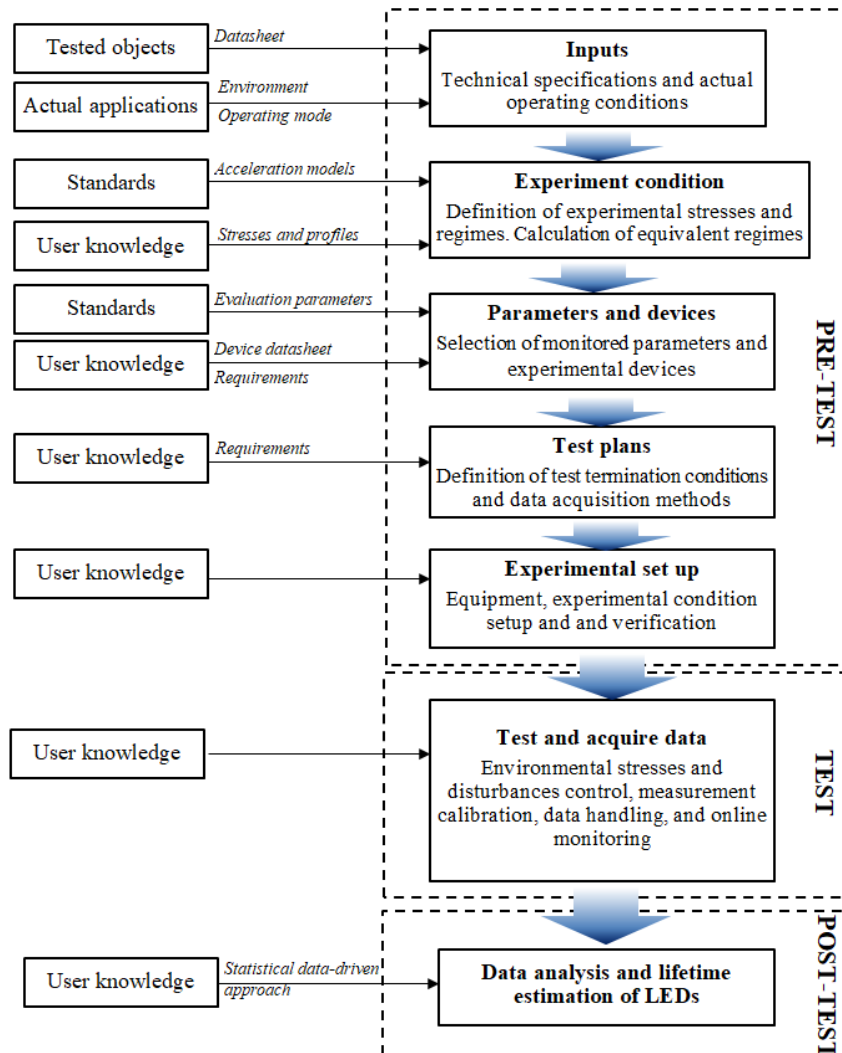


Fig. 1 Flowchart of the empirical approach for reliability estimation

## 2.1 Pre-Test Phase

The pre-test phase is essential in an experimental approach for lifetime estimation; because it ensures that the accelerated test conditions realistically represent the actual operating environment and produce meaningful reliability data. In this phase, infor-

mation from datasheets, real operating conditions, standards, and expert knowledge is used to select the dominant stress factors and the corresponding stress mode. The chosen stress must significantly impact degradation so that failures occur within practical test duration, while still preserving the real physical failure mechanisms.

Based on the selected stress, suitable acceleration models, such as Arrhenius, Eyring, Coffin-Manson, or inverse power law models, are determined [17]. These models convert real usage conditions into equivalent accelerated conditions, allowing the test to be shorter but still statistically representative of field operation (e.g., converting actual workload into equivalent test duty cycle or frequency). The relationship between the time under normal condition and the time under experimental condition is defined [17]:

$$t_U = t_T \cdot A_F \quad (1)$$

where  $A_F$  is the acceleration factor, which is calculated using various models such as Arrhenius, Eyring, Coffin-Manson, or inverse power law models depending on the type of stress,  $t_U$  and  $t_T$  are the operating times under normal condition and test.

Another key task is defining the degradation parameters to monitor. In ADT, this is crucial because the monitored parameter serves as the device's health indicator and directly reflects performance decline. This decision also determines the necessary measurement equipment and data acquisition setup.

Finally, an appropriate test plan must be designed. For non-repairable products like LEDs, common test plans are used depending on whether the time or number of failures is the stopping criterion. These plans ensure statistical validity, allow estimation of lifetime distributions, and provide enough data for model fitting and reliability prediction. Fig. 2 illustrates two test plans for unrepairable products, where  $n$  denotes the number of tested samples. The symbol  $U$  represents the action taken after a failure occurs, whereby the failed unit is removed from the testing process. The parameters  $\tau_0$  (planned test duration) and  $r_0$  (specified number of failures) define the criteria for terminating the test.

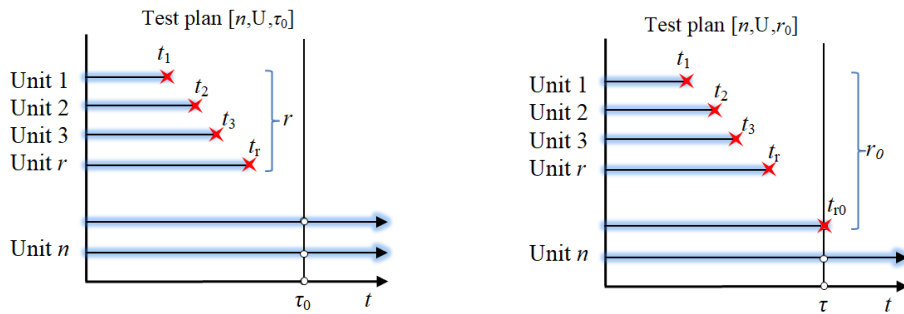


Fig. 2 Illustration of two test plans for unrepairable products

In summary, the pre-test phase defines the stress conditions, acceleration model, monitored parameters, and test plan. These elements are necessary to generate reliable, representative, and statistically useful degradation or failure data for lifetime estimation.

## 2.2 Practical Test Phase

The practical testing phase focuses on executing the accelerated test according to the predefined plan. In this phase, several issues must be carefully controlled to ensure

data validity. First, the test setup must guarantee stable stress conditions, such as temperature, current, humidity, or duty cycle, because fluctuations introduce uncertainty into degradation behavior. Second, the measurement system must be periodically calibrated to avoid drift, especially in long-term tests. Data sampling frequency is another important factor: low sampling may miss critical degradation events, while excessive sampling increases cost and noise.

Environmental disturbances, component variation, and certain unexpected failures (e.g., catastrophic failures unrelated to the target degradation mechanism) may also occur and must be recorded or filtered. Additionally, aging of auxiliary equipment (e.g., drivers, power supplies, sensors, or thermal chambers) can affect the results and requires scheduled maintenance. Throughout the test, data must be continuously monitored to detect anomalies, ensure reliability in acquisition, and to avoid data loss due to system interruptions. These considerations ensure that the collected data accurately reflects the degradation process and is suitable for subsequent lifetime estimation.

### 2.3 Post-Test Phase and Reliability Estimation

In the experimental approach for lifetime estimation, data collected during the testing phase must be processed using statistical, data-driven techniques to extract meaningful information about degradation and remaining useful life.

In ALT, only discrete failure-time data are typically available. Therefore, a statistical framework is required to estimate the reliability of the component based on these observed failure times. This forms an essential part of reliability engineering. First, the recorded failure times under stress conditions must be converted to equivalent times under normal operating conditions, using life-stress relationships such as those presented in Tab. 1. After the failure data are normalized, statistical methods are applied to model the underlying lifetime distribution of the LEDs. In this section, two core tasks will be carried out: (1) estimating the lifetime distribution of the LEDs, and (2) estimating the survival function and cumulative hazard function.

These contents are inherently related; once the lifetime distribution is identified, both the survival function and hazard function can be analytically determined. Two major methodological approaches are commonly used in this analysis: (1) non-parametric methods, which do not assume any predefined distribution, and (2) parametric methods, which assume that the failure times follow specific statistical distributions such as exponential, Weibull, lognormal, or gamma.

#### Non-Parametric Methods for Reliability Estimation

Non-parametric methods are appropriate when the underlying distribution of failure-time data is unknown. In this study, we introduce two approaches for estimating the lifetime characteristics of LEDs: (i) Kernel Density Estimation (KDE) for estimating PDF, and (ii) Kaplan-Meier estimation for the survival function. In addition, the cumulative hazard function is computed using the Nelson–Aalen estimator.

KDE is a non-parametric technique used to estimate the PDF of a random variable when the underlying distribution is unknown or uncertain [30]. Given a set of failure-time observations  $\mathbf{L} = (L_1, L_2, \dots, L_m)$ , the estimated density at a point  $l$  is computed as the average contribution of kernels centered at each data point. The estimator is defined as:

$$\hat{f}(l) = m^{-1}h^{-1} \sum_{i=1}^m K \frac{l - L_i}{h}, \quad -\infty < l < +\infty \quad (2)$$

where  $\hat{f}(y)$  denotes the estimated density at point  $l$ ;  $m$  is the number of observations of  $\mathbf{L}$ ;  $h$  is the bandwidth parameter that controls the smoothness of the density estimation;  $K(\bullet)$  is the kernel function, which is typically a symmetric PDF; and  $L_i$  represents each data point in the sample.

In practice, two key factors influence KDE performance: (i) Kernel selection and (ii) Bandwidth selection. While several kernel functions exist, Gaussian kernels are widely used due to their smoothness and strong theoretical foundation [31]. Although the kernel shape affects the result, the bandwidth  $h$  plays a significantly more critical role, as it determines the bias–variance trade-off and smoothness of the estimated density [31]. Common bandwidth selection methods include the rule-of-thumb approach, cross-validation, and the Sheather-Jones plug-in technique. However, KDE is only truly effective in the absence of censoring. When right-censored observations exist, KDE-based density estimation becomes biased unless specialized correction methods are applied.

For datasets with right-censoring, the Kaplan-Meier (KM) estimator is a more suitable approach, as it does not require any distributional assumptions. Let  $L_1 < L_2 < \dots < L_k$  denote the ordered failure times,  $d_i$  the number of observed failures at time  $t_i$ , and  $n_i$  the number of samples at risk just before time  $t_i$ . The KM estimate of the survival probability is defined as [32]:

$$\hat{S}(t) = \prod_{t_i \leq t} \left( 1 - \frac{d_i}{n_i} \right) \quad (3)$$

yielding a non-increasing, stepwise function that decreases only at observed failure times. The KM estimator provides an unbiased estimate of the survival function even in the presence of incomplete observations and is therefore widely applied in reliability analysis of engineering components.

Along with the survival probability, the cumulative hazard function is estimated using the Nelson–Aalen (NA) estimator. For the same ordered failure times  $t_i$ , the cumulative hazard is computed as [32]:

$$\hat{H}(t) = \sum_{t_i \leq t} \frac{d_i}{n_i} \quad (4)$$

Unlike the multiplicative form of the KM estimator, the NA estimator accumulates incremental hazard contributions additively. The estimate is monotonic and converges to the true cumulative hazard as the sample size increases. The survival function can also be recovered from the cumulative hazard function through:

$$\hat{S}(t) = \exp[-\hat{H}(t)] \quad (5)$$

offering an alternative, consistent representation of survivability.

Both KM and NA methods are fully non-parametric and therefore independent of any assumed lifetime distribution. While the KM estimator directly provides survival probabilities, the NA estimator yields a smoother cumulative hazard representation, especially for large datasets. When used together, these estimators provide a comprehensive description of LED reliability under accelerated testing conditions, including

both survival likelihood and failure accumulation rate.

### Parametric Methods for Reliability Estimation

In the parametric approach, the observed failure-time data are modelled using a suitable theoretical lifetime distribution such as the Weibull, Lognormal, Gamma, Exponential, or Normal distribution. Representative distributions commonly used in reliability analysis are summarized in Tab. 1.

Tab. 1 Some commonly used distributions [33]

Model	PDF	1 - CDF	Hazard	Parameter
Weibull	$\frac{a}{b} \left(\frac{t}{b}\right)^{a-1} \exp\left(-\left(\frac{t}{b}\right)^a\right)$	$\exp\left[-\left(\frac{t}{b}\right)^a\right]$	$\frac{a}{b} \left(\frac{t}{b}\right)^{a-1}$	Shape $a > 0$ Scale $b > 0$
Gamma	$\frac{\lambda}{\Gamma(a)} (\lambda t)^{a-1} \exp(-\lambda t)$	$\frac{\Gamma(a, \lambda t)}{\Gamma(a)}$	$\lambda(\lambda t)^{a-1} \frac{1}{\Gamma(a, \lambda t)} \exp(-\lambda t)$	Shape $a > 0$ Scale $\lambda > 0$
Lognormal	$\frac{1}{t\sigma} \phi(u), u = \frac{\log t - \mu}{\sigma}$	$1 - \Phi(u)$	$\frac{1}{t\sigma} \phi(u)$ $1 - \Phi(u)$	Mean $\mu \in (-\infty, +\infty)$ sdlog $\sigma > 0$

where  $\phi(u) = \frac{1}{\sqrt{2\pi}} \exp\left(-\frac{1}{2}u^2\right)$ ;  $\Phi(u) = \int_{-\infty}^u \phi(v) dv$ ;

$$\Gamma(a, x) = \int_0^\infty x^{a-1} \exp(-u) du, \Gamma(a) = \Gamma(a, 0), a > 0$$

The parameters of these distributions are typically estimated using Maximum Likelihood Estimation (MLE) or Bayesian inference. Once parameter estimates are obtained, goodness-of-fit tests and model selection criteria, such as the Anderson-Darling (AD) test, Akaike Information Criterion (AIC), and Bayesian Information Criterion (BIC), are applied to verify that the chosen distribution accurately represents the reliability characteristics of the LEDs.

The goodness-of-fit between the empirical failure-time data and a theoretical lifetime model is further evaluated using the AD statistical test. Unlike distance-based tests such as the Kolmogorov-Smirnov (KS) test, the AD test places greater emphasis on the tails of the distribution. This characteristic makes it particularly suitable for reliability studies, where early failures and late-life wear-out are of practical importance. Due to its sensitivity to tail behavior and strong performance for small or moderate sample sizes, the AD test is widely recommended for lifetime modelling.

For a sample of  $n$  ordered observations  $L_1 \leq L_2 \leq \dots \leq L_n$ , and assumed cumulative distribution function  $F(\cdot)$ , the AD test statistic is computed as [34]:

$$A^2 = -n - \sum_{i=1}^n \frac{2i-1}{n} \left\{ \ln[F(L_i)] + \ln[1-F(L_{n+1-i})] \right\} \quad (6)$$

A small value of  $A^2$  indicates that the observed data are closer to the assumed distribution, whereas a large value indicates poor fit.

While the AD test evaluates the statistical agreement between the model and the data, AIC and BIC quantify the trade-off between goodness-of-fit and model complexity. For a likelihood-based model with  $k$  estimated parameters and maximized

likelihood function  $LL$ , the criteria are defined as:

$$AIC = 2k - 2 \ln LL \quad (7)$$

$$BIC = k \ln n - 2 \ln LL \quad (8)$$

where  $n$  is the sample size. Lower AIC or BIC values indicate a better balance between fitting accuracy and parsimony. The AIC tends to favor more flexible models, whereas the BIC penalizes over-parameterization more strongly and is therefore more conservative.

By comparing AIC, BIC, and AD test statistics among candidate distributions, such as the Normal, Lognormal, Weibull, Gamma, and Exponential, the most appropriate lifetime distribution can be selected for subsequent reliability assessment. Once the model is established, reliability metrics such as the survival function, hazard function, MTTF, and confidence intervals can be analytically derived. This parametric framework enables robust reliability estimation even when ALT provides only limited or highly accelerated information.

### 3 Case Study

In this study, an accelerated test was conducted on 20 high-power 10 W LEDs (700 lm, 90 °C) [35]. The key specifications of the LEDs are summarized in Tab. 2. Although these devices are commercial products, they satisfy typical military requirements, including long operational lifetime, high reliability, compact structure, high luminous output, and ease of replacement.

Tab. 2 Parameters of LED 10W 700LM/90°C [35]

Parameters	Values	Units
Luminous flux	700–800	lm
Correlated Color Temperature	2 900–3 200	K
Forward Voltage	9–11	V
Maximum Forward Current	1 050	mA
Thermal Resistance	12	°C/W
Junction temperature	115	°C
Operating temperature	–40 to +60	°C

#### 3.1 Experimental Set Up

The assumed application is an interior lighting system of military vehicles or lighting systems in the barracks, where the typical operating temperature is +24 °C and frequent ON/OFF switching occurs during missions. Preliminary analysis showed that ON/OFF cycling is one of the dominant factors influencing LED lifetime. Based on the expected working environment and switching behavior, an accelerated test was designed with thermal stress as the acceleration factor, and the Arrhenius acceleration model was selected as appropriate. Considering the manufacturer's datasheet limits, the test temperature was set to +90 °C, approximately 10 °C below the maximum junction temperature and higher than maximum operating temperature. The LEDs were operated in a cyclic ON/OFF mode with a maximum driving current of 1 050 mA,

which corresponds to the rated operating current. Thus, the acceleration factor of the test is determined by the shortened form of the Arrhenius equation [17]:

$$A_F = 2^{\frac{\Delta T}{10}} = 2^{\frac{T_T - T_U}{10}} = 2^{\frac{90 - 24}{10}} \approx 97 \quad (9)$$

We assume that the LEDs are switched approximately 15 times per day, with similar ON and OFF durations. This corresponds to an ON duration of 48 minutes in each cycle. Under the Arrhenius-based acceleration regime, the ON/OFF time in the accelerated test was shortened to 30 seconds per state, resulting in one switching cycle per minute. The complete test mode is shown in Tab. 3. Since the objective is to obtain lifetime data, the test was continued until all LEDs failed. In addition to recording failure times, forward voltage was monitored throughout the experiment and used as degradation data for additional analysis.

Tab. 3 Experimental condition in ALTs for tested LED

Parameters	Values
Current level ( $I_T$ )	1 050 mA
Temperature ( $T_T$ )	+90 °C
Switching frequency in ALTs	1 time/min
Operation time in each cycle	30 s
Non-operation time in each cycle	30 s

The experiment was carried out using a VC3-7034 thermal chamber to control the thermal environment. High-precision DC power supplies provided stable current to the LEDs. A high-sensitivity Agilent data acquisition system continuously recorded voltage signals. All equipment was controlled and monitored through a central computer. The overall test rig is illustrated in Fig. 3.

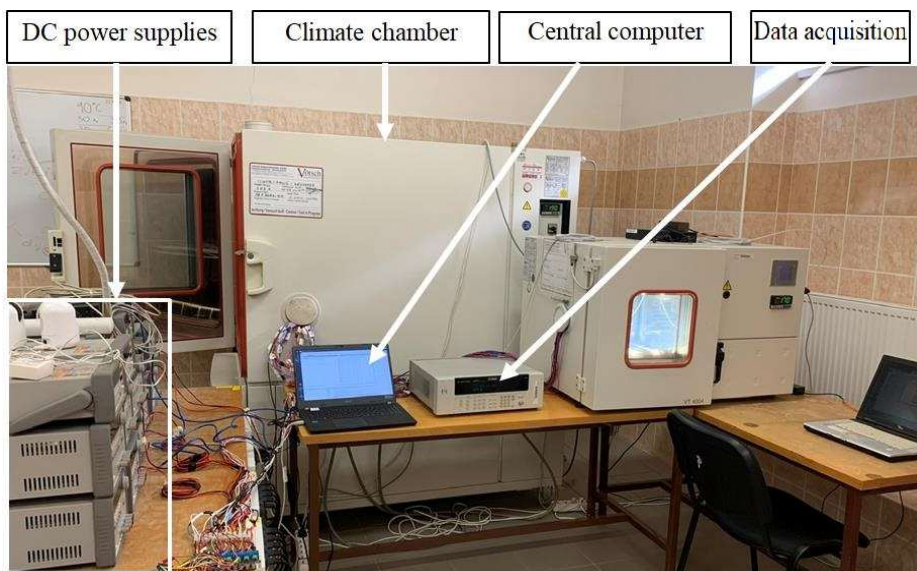


Fig. 3 Test rig for LED 10W 700LM/90 °C

### 3.2 Experimental Data

We conducted the test and continuously monitored the forward voltage of the LEDs. Measurements were recorded every 5 min, providing a sufficiently large dataset for degradation analysis and reliability prediction. Tab. 4 illustrates a sample of the recorded voltage data.

Tab. 4 Example of the raw voltage degradation data of LEDs from ATs

Time [min]	Voltage [V] /LED1001	Voltage [V] /LED1002	Voltage [V] /LED1003	...	Voltage [V] /LED1020
0	8.6542454	8.7043258	8.6994052	...	8.6701461
5	8.6537288	8.7038502	8.6988722	...	8.6689570
10	8.6535156	8.7036616	8.6987656	...	8.6684978
15	8.6538436	8.7039322	8.6989706	...	8.6683420
20	8.6541552	8.7042438	8.6992330	...	8.6685716
...	...	...	...	...	...

To ensure the reliability of the measured LED voltage, we evaluated both the measurement uncertainty and the statistical characteristics of the recorded data. The measurement uncertainty is quantified following the Type B evaluation procedure recommended in JCGM 100:2008 [36], based on the technical specifications of the Keysight 34980A with the 34922A multiplexer module [37] employed for data acquisition. The resulting standard uncertainty is 0.208 mV, corresponding to an expanded uncertainty of 0.416 mV ( $k = 2$ ) at the maximum measured voltage (~9 V). This uncertainty is negligible compared with the substantial voltage increases (typically tens of percent) that indicate LED malfunction [35]. We also performed both AD and KS tests to characterize data behavior. The results indicate that the measured voltage data do not follow standard theoretical distributions such as normal, Weibull, gamma, or lognormal. This behavior is expected in the experiments [38]. Nonetheless, these tests are used solely to assess data quality rather than to impose parametric assumptions.

Based on the above assessment, a fully non-parametric analysis procedure is adopted, including moving-average smoothing [39], modified Akima cubic interpolation [40], and At-Most-One-Changepoint detection (AMOC) [33] to detect data structural changes and identify failure. This approach does not assume any underlying data distribution, ensuring that the analysis remains valid even when the measured voltages deviate from standard theoretical models and is not affected by measurement uncertainty.

Fig. 4 shows the voltage degradation curves of 20 LEDs until failure. The left plot displays the raw voltage trajectories, while the right plot shows the smoothed and outlier-filtered curves obtained using a moving-average method combined with Modified Akima cubic interpolation.

Sudden voltage drops observed in the raw data (Fig. 4, left) are considered outliers, primarily caused by measurement noise, random fluctuations, or transient effects associated with ON/OFF switching in testing condition of LEDs. These outliers do not reflect the actual long-term degradation of the LEDs and are therefore excluded from the smoothed trend to provide a more accurate representation of the degradation path.

In contrast, significant voltage increases correspond to structural changes in the data and are directly related to failure events [33]. Distinguishing between these two types of variations ensures that the smoothing process preserves meaningful signals for failure detection while filtering irrelevant noise.

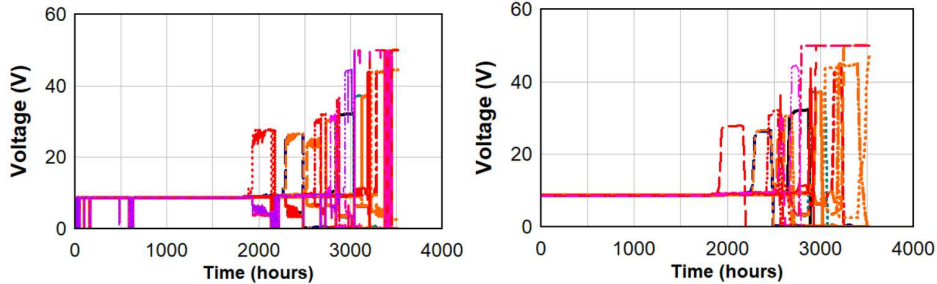


*Fig. 4 Graphical plots of raw voltage degradation paths (left) and smoothed paths (right) using moving-average method and Modified Akima cubic interpolation of tested LEDs*

From the degradation curves, it can be observed that LED failure is generally characterized by a sudden increase in forward voltage. This behavior is used as the degradation signature to detect failures. However, to determine the failure time more accurately and objectively, we applied a data-structure analysis based on the AMOC approach, specifically the AMOC-mean-var-mean-var method [33]. Tab. 5 reports the observed failure times obtained using AMOC, together with the equivalent failure times adjusted to normal operating conditions using the Arrhenius acceleration model. It should be noted that the failures identified here are complete failures, meaning that the LEDs stop functioning. The Arrhenius-adjusted lifetimes are considered as the effective lifetimes under normal conditions and are used in the subsequent analysis.

*Tab. 5 Failure time of LEDs in test and adjusted equivalent failure time in normal operating conditions using Arrhenius equation*

No. LED	Failure time in ALT [h]	Equivalent failure time [h]	No. LED	Failure time in ALT [h]	Equivalent failure time [h]
1 001	2 757.12	267 456.80	1 011	2 206.08	214 002.69
1 002	2 186.40	212 093.61	1 012	3 141.12	304 707.05
1 003	2 761.20	267 852.58	1 013	2 766.96	268 411.34
1 004	3 023.04	293 252.60	1 014	2 332.08	226 225.43
1 005	3 098.64	300 586.24	1 015	2 808.48	272 439.02
1 006	3 049.20	295 790.27	1 016	1 864.08	180 826.68
1 007	2 509.92	243 476.95	1 017	2 763.12	268 038.83
1 008	3 054.00	296 255.90	1 018	2 734.08	265 221.78
1 009	2 442.00	236 888.31	1 019	2 463.12	238 937.07
1 010	3 137.04	304 311.26	1 020	2 635.92	255 699.69

### 3.3 Reliability Estimation

In this section, the lifetime of LEDs, along with their survival and cumulative hazard functions, is estimated using both non-parametric and parametric methods described in Section 2.3, based on the failure time data in Tab. 5. For the non-parametric approach, Gaussian kernel with Sheather-Jones plug-in bandwidth selection is employed to estimate the lifetime distribution using KDE, while Kaplan-Meier and Nelson-Aalen methods are applied to derive the survival functions and cumulative hazard functions. In the parametric approach, widely used distributions including Weibull, Gamma, and log-normal are fitted to the lifetime data. Parameters are estimated using MLE, and the goodness-of-fit is assessed through AD tests as well as AIC and BIC criteria. The survival and cumulative hazard functions are subsequently derived from the corresponding CDFs and PDFs.

Tabs 6 and 7 summarize the MLE parameter estimates and the results of goodness-of-fit evaluation, respectively. Figs 5 and 6 provide graphical representations of the lifetime CDFs, PDFs, survival functions, and cumulative hazard functions obtained from both non-parametric and parametric analyses. The results indicate that both approaches yield consistent and reliable estimates of LED lifetime and reliability metrics. Among the parametric models, the Weibull distribution demonstrates the best fit, as supported by AD test, AIC, and BIC values in Tab. 7.

Tab. 6 Parameter estimation results of Weibull, Gamma and log-normal distributions for LEDs lifetime based on MLE

Weibull		Gamma		Log-normal	
$a$	$b$	$a$	$b$	$\mu$	$\sigma$
$2.7496 \times 10^5$	9.6028	12.4618	0.1370	55.5443	$4.6922 \times 10^3$

Tab. 7 Goodness-of-fit results of the parametric lifetime models for LEDs using AD test, AIC and BIC

Distribution	Weibull	Gamma	Log-normal
AD	<b>0.4169</b>	0.5184	0.5481
AIC	<b>476.02</b>	479.01	479.75
BIC	<b>478.01</b>	481.00	481.74

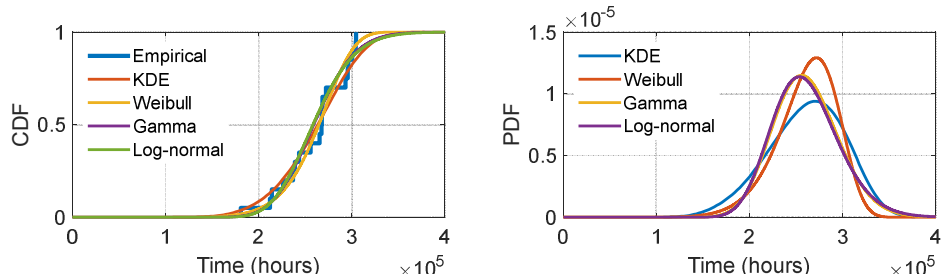


Fig. 5 Graphical plots of CDF (left) and PDF (right) of lifetime using non-parametric and parametric methods

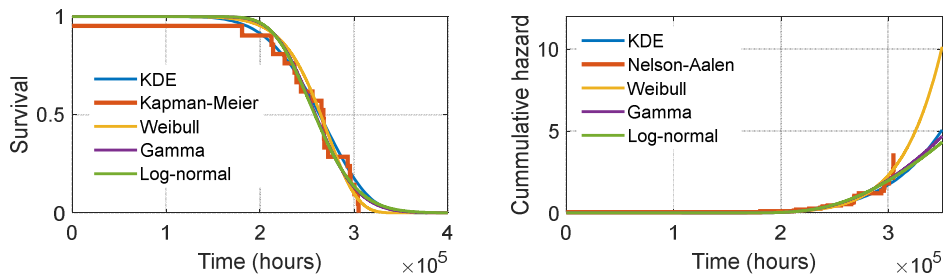


Fig. 6 Graphical plots of survival functions and cumulative hazard functions of LEDs using non-parametric and parametric methods

Such reliability estimation is particularly important in practical applications, especially for military equipment where spare parts and replacements may be limited. Tab. 8 further provides critical operating times and corresponding failure rates of the tested LEDs, offering essential information for maintenance planning, stocking replacement components, and supporting operational readiness.

Tab. 8 Critical operating times and corresponding failure rates of tested LEDs

Failure probability	Empirical [h]	KDE [h]	Weibull [h]	Gamma [h]	Log-Normal [h]
0.05	196 460.1	172 924.5	201 806.3	205 891.7	204 961.2
0.10	213 048.2	187 112.4	217 515.1	216 932.4	215 700.9
0.25	237 912.7	210 427.8	241 500.1	236 262.9	234 916.8
0.50	267 654.7	232 949.2	264 659.9	259 061.3	258 281.2
0.75	294 521.4	249 350.0	284 469.9	283 282.0	283 969.3
0.90	302 448.8	257 951.6	299 905.1	306 323.7	309 267.0
0.95	304 509.2	260 705.2	308 237.4	320 685.6	325 472.1

### 3.4 Discussion

The experimental results and reliability estimation outcomes obtained in this case study demonstrate that the proposed approach provides accurate and robust estimation performance. The tests delivered not only failure observations but also continuous degradation data, enabling precise determination of failure times through data-structure analysis methods, as presented in Section 3.2. It is also important to emphasize the advantages of accelerated testing in reliability studies. A major benefit is the significant reduction in testing duration while still reproducing realistic operating conditions. In this study, the overall test period was shortened by approximately a factor of 100 compared with normal-use conditions, while preserving high-quality, long time-series data. However, accelerated testing requires appropriate equipment and a clear understanding of the actual operating environment to ensure meaningful stress selection and a suitable acceleration model.

It can be observed that the lifetime distribution, survival function, and cumulative hazard function were estimated with high accuracy using both parametric and nonparametric statistical techniques, as illustrated in Figs 5 and 6. Additionally, the approach

provides practical information on operating time and corresponding failure severity (Tab. 8), which is essential for maintenance planning, repair scheduling, and spare-part provisioning.

Among the evaluated statistical models, the non-parametric nonlinear KDE method yields lower estimate performance, whereas the parametric models produce relatively consistent results. The Weibull distribution exhibits the closest agreement with the experimental data. Therefore, the Weibull distribution is the most suitable parametric model in this case. Nonetheless, a limitation of these approaches is that they rely on actual failure events; therefore, ALTs may still require long test durations. In some applications, ADT offers a more suitable alternative, as it enables reliability prediction even in the absence of failures and supports real-time condition-based estimation, an increasingly important requirement in modern reliability engineering. The development of degradation-based predictive methods falls outside the scope of this paper and will be addressed in future work.

## 4 Conclusions

In this paper, we analyzed the reliability requirements of military equipment, focusing on LEDs as critical components. We reviewed methods for evaluating LED reliability and predicting their lifetime, highlighting the importance of reliability testing, particularly accelerated testing, and data-driven approaches for modelling and prediction. We proposed an experimental methodology for LED reliability assessment, structured as a stepwise process that defines stress selection, test regimes, equipment, and data processing strategies.

To demonstrate the approach, an accelerated reliability test was conducted on LEDs that meet military requirements under realistic operating conditions and modes. Both degradation and failure-time data were collected, with failure times determined using advanced data analysis techniques. Parametric and non-parametric statistical methods were applied to estimate lifetime distributions, survival functions, and cumulative hazard functions. The results also provided practical information on operating time and failure levels, supporting maintenance planning, inventory management, and operational readiness.

Future work will extend accelerated testing to varied operating conditions and modes, with a focus on collecting degradation data and developing online, data-driven methods for real-time reliability estimation, a critical aspect for high-reliability military applications.

## Acknowledgement

The paper has been prepared with the support of the Ministry of Defence of the Czech Republic – Project for the Development of the Organization DZRO VAROPS and Specific Research Project SV22-202.

## References

- [1] MIL-STD-810H:2019, *Department of Defense Test Method Standard: Environmental Engineering Considerations and Laboratory Tests*.
- [2] MIL-STD-883L:2019, *Department of Defense Test Method Standard for Microcircuits*.

- [3] MIL-STD-785B:1980, *Military Standard: Reliability Program for Systems and Equipment Development and Production*.
- [4] MIL-STD-781A:1996, *Military Handbook: Reliability Test Methods, Plans, and Environments for Engineering Development, Qualification, and Production*.
- [5] IEC 60300:2023, *Dependability Management*.
- [6] MIL-HDBK-217F:1991, *Military Standard: Reliability Prediction of Electronic Equipment*.
- [7] IEEE 1413:2010, *IEEE Standard Framework for Reliability Prediction of Hardware*.
- [8] O'CONNOR, P. and A. KLEYNER. *Practical Reliability Engineering*. 5<sup>th</sup> ed. New York: Wiley, 2012. ISBN 1-119-96126-2.
- [9] CU, X.P. and H.A. BUI. Methodologies for Reliability Prediction of Electronic Component in Military Vehicles. *Advances in Military Technology*, 2019, **14**(1), pp. 89-98. DOI 10.3849/aimt.01276.
- [10] KYATAM, S., L.N. ALVES, S. MASLOVSKI and J.C. MENDES. Impact of Die Carrier on Reliability of Power LEDs. *Journal of the Electron Devices Society*, 2021, **9**, pp. 854-863. DOI 10.1109/JEDS.2021.3115027.
- [11] TSAI, Y.C., J.P. LEBURTON and C. BAYRAM. Quenching of the Efficiency Droop in Cubic Phase InGaAlN Light-Emitting Diodes. *IEEE Transactions on Electron Devices*, 2022, **69**(6), pp. 3240-3245. DOI 10.1109/TED.2022.3167645.
- [12] NELSON, W.B. *Accelerated Testing: Statistical Models, Test Plans, and Data Analysis*. New York: Wiley, 2009. ISBN 978-0-4703-1679-5.
- [13] IEC 62506:2023, *Methods for Product Accelerated Testing*.
- [14] IES LM-80-08:2008, *Approved Method: Measuring Lumen Maintenance of LED Light Sources*.
- [15] IES TM-21-11:2011, *Projecting Long-Term Lumen Maintenance of LED Light Sources*.
- [16] LIMON, S., O.P. YADAV and H. LIAO. A Literature Review on Planning and Analysis of Accelerated Testing for Reliability Assessment. *Quality and Reliability Engineering International*, 2017, **33**(8), pp. 2361-2383. DOI 10.1002/qre.2195.
- [17] *Accelerated Life Testing Data Analysis Reference* [online]. Tucson: ReliaSoft, 2024 [viewed 2025-10-10]. Available from: [https://help.reliasoft.com/reference/accelerated\\_life\\_testing\\_data\\_analysis/pdfs/alt\\_ref.pdf](https://help.reliasoft.com/reference/accelerated_life_testing_data_analysis/pdfs/alt_ref.pdf)
- [18] HERZOG, A., et al. Long-Term Temperature-Dependent Degradation of 175 W Chip-on-Board LED Modules. *IEEE Transactions on Electron Devices*, 2022, **69**(12), pp. 6830-6836. DOI 10.1109/TED.2022.3214169.
- [19] SINGH, P. and C. TAN. Degradation Physics of High Power LEDs in Outdoor Environment and the Role of Phosphor in the Degradation Process. *Scientific Reports*, 2016, **6**, 24052. DOI 10.1038/srep24052.
- [20] TRUONG, M.T., P. DO, L. MENDIZABAL and B. IUNG. An Improved Accelerated Degradation Model for Led Reliability Assessment with Self-Heating Impacts. *Microelectronics Reliability*. 2022, **128**, 114428. DOI 10.1016/j.microrel.2021.114428.
- [21] CHOI, H., L. WANG, S.W. KANG, J. LIM and J. CHOI. Precise Measurement of Junction Temperature by Thermal Analysis of Light-Emitting Diode Operated

- at High Environmental Temperature. *Microelectronics Reliability*, 2021, **235**, 111451. DOI 10.1016/j.mee.2020.111451.
- [22] IBRAHIM, M.S., J. FAN, W.K. YUNG, Z. JING, X. FAN, W. VAN DRIEL and G. ZHANG. System Level Reliability Assessment for High Power Light-Emitting Diode Lamp Based on a Bayesian Network Method. *Measurement*, 2021, **176**, 109191. DOI 10.1016/j.measurement.2021.109191.
- [23] VALIŠ, D., M. FORBELSKÁ, Z. VINTR, Q.T. LA and J. LEUCHTER. Perspective Estimation of Light Emitting Diode Reliability Measures Based on Multiply Accelerated Long Run Stress Testing Backed Up by Stochastic Diffusion Process. *Measurement*, 2023, **206**, 112222. DOI 10.1016/j.measurement.2022.112222.
- [24] DO, G.H., S.J. LEE, J.S. KIM and J.Y. KIM. Development of Accelerated Life Testing Apparatus for Light-Emitting Diode Therapy. *IEEE Transactions on Device and Materials Reliability*, 2021, **21**(4), pp. 608-612. DOI 10.1109/TDMR.2021.3121387.
- [25] WANG, Y., et al. Gamma-Irradiation-Accelerated Degradation in AlGaN-Based UVC LEDs Under Electrical Stress. *IEEE Transactions on Nuclear Science*, 2021, **68**(2), pp. 149-155. DOI 10.1109/TNS.2020.3046255.
- [26] TAN, K.Z., S.K. LEE and H.C. LOW. LED Lifetime Prediction Under Thermal-Electrical Stress. *IEEE Transactions on Device and Materials Reliability*, 2021, **21**(3), pp. 310-319. DOI 10.1109/TDMR.2021.3085579.
- [27] ENAYATI, J., A. RAHIMNEJAD and S.A. GADSDEN. LED Reliability Assessment Using a Novel Monte Carlo-Based Algorithm. *IEEE Transactions on Device and Materials Reliability*, 2021, **21**(3), pp. 338-347. DOI 10.1109/TDMR.2021.3095244.
- [28] HOANG, A.D., Z. VINTR, D. VALIS and D. MAZURKIEWICZ. An Approach in Determining the Critical Level of Degradation Based on Results of Accelerated Test. *Eksplotacja i Niezawodność – Maintenance and Reliability*, 2022, **24**(2), pp. 330-337. DOI 10.17531/ein.2022.2.14.
- [29] LETSON, B.C., S. BARKE, P. WASS, G. MUELLER, F. REN, S.J. PEARTON and J.W. CONKLIN. Deep UV AlGaN LED Reliability for Long Duration Space Missions. *Journal of Vacuum Science & Technology A*, 2023, **41**(1), 013202. DOI 10.1116/6.0002199.
- [30] CHEN, Y.C. A Tutorial on Kernel Density Estimation and Recent Advances. *Biostatistics & Epidemiology*, 2017, **1**(1), pp. 161-187. DOI 10.1080/24709360.2017.1396742.
- [31] SILVERMAN B.W. *Density Estimation: for Statistics and Data Analysis*. London: Chapman and Hall, 1986. ISBN 978-1-3151-4091-9.
- [32] COLOSIMO, E., F.V. FERREIRA, M. OLIVEIRA and C. SOUSA. Empirical Comparisons Between Kaplan-Meier and Nelson-Aalen Survival Function Estimators. *Journal of Statistical Computation and Simulation*, 2022, **72**(4), pp. 299-308. DOI 10.1080/00949650212847.
- [33] VALIŠ, D., M. FORBELSKÁ, Z. VINTR, Q.T. LA and Z. KOHL. Light Emitting Diode Degradation and Failure Occurrence Modelling Based on Accelerated Life Test. *Engineering Failure Analysis*, 2025, **169**, 109200. DOI

- 10.1016/j.engfailanal.2024.109200.
- [34] DARLING, D.A. and T.W. ANDERSON. Asymptotic Theory of Certain Goodness-of-Fit Criteria Based on Stochastic Processes. *The Annals of Mathematical Statistics*, 1952, **23**(2), pp. 193-212. DOI 10.1214/aoms/1177729437.
  - [35] *Specification for Approval for LED GT-P10WW339910700*. China: ShenZen GeTian Optoelectronics Co., 2013.
  - [36] JCGM 100:2008, *Evaluation of Measurement Data: Guide to the Expression of Uncertainty in Measurement*.
  - [37] 34980A Data Acquisition System [online]. 2019 [viewed 2025-11-12]. Available from: <https://www.keysight.com/zz/en/assets/7018-01247/data-sheets/5989-1437.pdf>
  - [38] SAINANI, K.L. Dealing with Non-Normal Data. *Physical Medicine and Rehabilitation*, 2012, **4**(12), pp. 1001-1005. DOI 10.1016/j.pmrj.2012.10.013.
  - [39] MOLUGARAM, K. and G.S. RAO. Analysis of Time Series. In: *Statistical Techniques for Transportation Engineering*. Oxford: Butterworth-Heinemann, 2017, pp. 463-489. DOI 10.1016/B978-0-12-811555-8.00012-X.
  - [40] REN, K., M. ALAM, P.P. NIELSEN, M. GUSSMANN and L. RÖNNEGÅRD. Interpolation Methods to Improve Data Quality of Indoor Positioning Data for Dairy Cattle. *Frontiers in Animal Science*, 2022, **3**, 896666. DOI 10.3389/fanim.2022.896666.